https://doi.org/10.5194/ar-2026-23
Preprint. Discussion started: 24 June 2026

AEROSOL Research Discussions

Role of Methanesulfonic Acid in Freshly Nucleated Particle Formation and Growth

Galib Hasan, Yosef Knattrup, Haide Wu, and Jonas Elm
Department of Chemistry, Aarhus University, Langelandsgade 140, 8000 Aarhus C, Denmark
Correspondence: Jonas Elm (jelm@chem.au.dk)

Abstract.

Sulfuric acid (SA) together with base molecules such as ammonia (AM), methylamine (MA) and dimethylamine (DMA) is known to play a central role in atmospheric new particle formation (NPF). NPF occurs through gas-to-particle conversion via the formation and growth of molecular clusters. While previous studies have demonstrated that mixtures of bases can strongly enhance nucleation rates, the influence of multiple acidic species for larger cluster stability and growth remains less explored.

In this work, we investigate the role of mixed-acid systems in atmospheric cluster formation using quantum chemical calculations, assisted by machine-learning. Cluster structures containing SA, methane sulfonic acid (MSA), and atmospherically relevant bases (AM, MA, and DMA), with compositions up to 10 acid–base pairs, were generated through extensive configurational sampling using ABCluster and metadynamics simulations with CREST. The resulting structures were subsequently optimized at the B97-3c level of theory, while a PaiNN machine-learning model was used to accelerate the calculation.

Our results show that, in contrast to previously reported base synergy, the acid synergy between SA and MSA is weak and highly system dependent. SA consistently dominates the thermodynamic stability of the smallest clusters, and MSA-only acid–base interactions are insufficient to explain efficient initial particle formation. In particular, for systems involving DMA, the strong SA–DMA interaction governs the cluster energetics, with little contribution of MSA to the stability. However, MSA can influence cluster stability at larger sizes in systems involving weaker bases such as AM and MA, especially under conditions where the relative abundance of MSA is high. These findings indicate that MSA does not act as a primary nucleating acid, but rather as a secondary species that participate in the early growth of clusters.

Overall, this work highlights that the roles of different atmospheric acids in NPF are fundamentally distinct: SA controls the initial nucleation step, whereas MSA may enhance subsequent cluster growth under specific atmospheric conditions.

1 Introduction

Atmospheric aerosol particles play a central role in air quality and climate. Aerosols originate from both primary emissions and secondary formation processes. While primary aerosols are emitted directly into the atmosphere, secondary aerosols are formed through gas-to-particle conversion processes that can produce freshly nucleated particles (FNPs). The initial step of this process involves the formation of molecular clusters stabilized by strong hydrogen-bonding interactions between atmospheric

https://doi.org/10.5194/ar-2026-23
Preprint. Discussion started: 24 June 2026

AEROSOL Research Discussions

vapors (Kulmala et al., 2013). Clusters that are sufficiently stable against evaporation can grow through condensation and coagulation processes, eventually forming particles with diameters exceeding roughly 2 nm.

Fine particles (<1 μm) and ultrafine particles (<100 nm) are particularly important due to their impacts on both human health and the Earth's radiative balance. Fine particulate matter is one of the leading contributors to air pollution-related mortality worldwide (Pelucchi et al., 2009; Cromar and Lazrak, 2023). In addition to their health effects, aerosols influence climate directly by scattering and absorbing solar radiation and indirectly by acting as cloud condensation nuclei (CCN), thereby affecting cloud formation and properties (Loeb and Kato, 2002; Rosenfeld et al., 2014; Zhao et al., 2024). Despite their importance, aerosol–cloud interactions remain one of the largest uncertainties in current climate models (Cooley et al., 2023).

Inorganic acids and bases are widely recognized as key contributors in the initial steps of cluster formation. Sulfuric acid (SA), together with bases such as ammonia (AM) and amines, constitutes one of the most important nucleation pathways in many atmospheric environments (Spracklen et al., 2006; Sipilä et al., 2010; Kirkby et al., 2011b; Almeida et al., 2013). Other atmospheric components may further influence these processes, including ions produced by galactic cosmic rays (Kirkby et al., 2016, 2011a) and highly oxygenated organic molecules (HOMs) (Bianchi et al., 2016; Schobesberger et al., 2013; Riccobono et al., 2014). Understanding new particle formation (NPF) therefore requires detailed knowledge of both the chemical composition of clusters and the concentrations of their precursor vapors.

Experimental characterization of clusters smaller than 2nm remains extremely challenging. Conventional condensation particle counters (CPCs) have detection limits of approximately 2–3 nm, which prevents direct observation of the smallest clusters (McMurry, 2000). Particle size magnifiers (PSMs) can go down to around $\sim$1.5 nm, but they provide limited chemical information about cluster chemical composition (Vanhanen et al., 2011). Techniques such as chemical ionization atmospheric pressure interface time-of-flight mass spectrometer (CI-APi-TOF) have enabled detailed investigation of cluster composition (Jokinen et al., 2012). However, they can easily alter cluster structures during ionization due to fragmentation effects (Zapadinsky et al., 2018; Passananti et al., 2019; Alfaouri et al., 2022). Moreover, these measurements are typically limited to clusters containing up to roughly ten acid and base molecules Almeida et al. (2013). As a result, the chemical composition and stability of clusters in the size range between approximately 1.0 and 2.0 nm remain poorly understood. This size regime is particularly important because it corresponds to the transition from molecular clusters to stable aerosol particles (Kulmala et al., 2013; Wu et al., 2024). Computational approaches have therefore become essential for bridging this gap. For example, Wu et al. (2023) introduced a framework that enables systematic exploration of atmospheric cluster formation from individual molecules to clusters approaching 2 nm in size. Such methods allow detailed investigation of cluster thermodynamics, intermolecular interactions, and growth pathways, providing insights into the mechanisms governing the formation of atmospheric freshly nucleated particles (FNPs).

AM and amines are emitted from a wide range of anthropogenic and natural sources, including agriculture, industrial activities, combustion processes, and marine environment (Ge et al., 2011). Among these, AM, methylamine (MA) and dimethylamine (DMA) play a particularly important role in enhancing SA-driven nucleation, significantly increasing particle formation rates compared to pure SA or SA–water systems (Sipilä et al., 2010; Almeida et al., 2013). This enhancement arises from pro-

https://doi.org/10.5194/ar-2026-23
Preprint. Discussion started: 24 June 2026

AEROSOL Research Discussions

ton transfer reactions between acids and bases, leading to salt formation and increased cluster stability. Numerous quantum chemical studies have confirmed the stabilizing effect of AM (Ianni and Bandy, 1999; Larson et al., 1999; Nadykto and Yu, 2007; Kurt'en et al., 2007; Loukonen et al., 2010; Herb et al., 2011; DePalma et al., 2012, 2014), MA (Nadykto et al., 2011, 2014b, 2015), and DMA (Kurtén et al., 2008; Loukonen et al., 2010; Kupiainen-Mä"attä et al., 2012; Ortega et al., 2012; Olenius et al., 2013; Nadykto et al., 2014a; Henschel et al., 2014; DePalma et al., 2012, 2014; Henschel et al., 2016; Ma et al., 2016) in stabilizing initial SA clusters.

Methanesulfonic acid (MSA), which is frequently observed in atmospheric aerosol particles, has been proposed as an important contributor to NPF alongside SA (Sorooshian et al., 2009; Facchini et al., 2008). MSA is primarily produced through the oxidation of organosulfur compounds, often concurrently with SO_2 (the main precursor of SA), from sources such as marine biological activity, biomass burning, and industrial emissions (Bates et al., 1992; VanderGheynst et al., 1998; Rosenfeld et al., 2001; Meinardi et al., 2003; Barnes et al., 2006). Typical atmospheric gas-phase concentrations of MSA are on the order of $\sim 10^5$–10^7 molecules cm^{-3}, corresponding to approximately 10–100 % of SA concentrations (Eisele and Tanner, 1993; Napari et al., 2002).

Both experimental and theoretical studies have demonstrated that MSA can participate in cluster formation with bases such as AM and amines (Shen et al., 2019, 2020; Liu et al., 2022), particularly under conditions where SA concentrations are limited. Recent computational studies have further highlighted the role of MSA in stabilizing acid–base clusters and influencing their growth pathways, suggesting that its contribution to NPF may be more significant than previously assumed (Shen et al., 2019, 2020; Liu et al., 2022).

Despite these advances, the molecular-level understanding of large clusters involving both SA and MSA remains limited. In particular, the synergistic effects between different acids in stabilizing molecular clusters and promoting their growth are still not well understood. This gap highlights the need for systematic molecular-level investigations of mixed-acid systems under atmospherically relevant conditions.

In this work, we address this challenge by extending computational investigations to chemically complex mixed-acid–base clusters. Specifically, we perform quantum chemical calculations on clusters of the form $(MSA)_n(base)_n$ and $(SA)_{n-1}(MSA)_1(base)_n$, considering systems up to $n = 10$ acid-base molecules.

2 Methods

2.1 Computational details

Density functional theory calculations used during the configurational sampling workflow — including single-point energies, geometry optimizations, and vibrational frequency calculations — were carried out with the empirically corrected B97-3c method (Brandenburg et al., 2018) as implemented in the ORCA 5.0.4 quantum chemistry package (Neese, 2022). Semi-empirical calculations were performed with the xTB 6.4.0 program (Bannwarth et al., 2021) using both the original GFN1-xTB method (Grimme et al., 2017) and a reparameterized variant, GFN1-xTB$^{re\text{-}par}$, developed by Knattrup et al. (2024) on the basis of previously reported FNP structures (Wu et al., 2024). Initial cluster geometries were generated with ABCluster

https://doi.org/10.5194/ar-2026-23
Preprint. Discussion started: 24 June 2026

AEROSOL Research Discussions

version 3.2 (Zhang and Dolg, 2015, 2016) employing the CHARMM force field (Huang and MacKerell Jr, 2013). Additional conformational exploration was performed using CREST in non-covalent interaction mode through metadynamics simulations (Pracht et al., 2017, 2020; Pracht and Grimme, 2021; Grimme, 2019; Spicher et al., 2022).

2.2 Configurational sampling of $(MSA)_1(SA)_{n-1}(AM/MA/DMA)n$, with $n = 1 - 5$ clusters

We initially studied $(MSA)_1(SA)_{n-1}(AM/MA/DMA)_n$ clusters of 1 to $n = 5$ acid molecules. The configurational sampling of the clusters were performed using our recently developed improved configuration sampling workflow (Wu et al., 2023, 2024). The configurational sampling procedure can be outlined as follows:

$$\text{ABC} \xrightarrow{N=10{,}000} \text{xTB}^{\text{OPT}} \xrightarrow{N=10{,}000} \text{B97-3c}^{\text{SP}} \xrightarrow[\text{filter}]{N=1{,}000} \text{B97-3c}^{\text{PART OPT}} \xrightarrow[\text{filter}]{N=100} \text{B97-3c}^{\text{FULL OPT}} \qquad \text{(ABC track)}$$

Initial cluster geometries were generated using 10 parallel ABCluster runs, generating 10,000 local minimum configurations. Previous works (Wu et al., 2023, 2024) have shown that performing several parallel ABCluster searches improves finding global minimum of large molecular clusters compared with a single extended search. Ionic monomers were employed while maintaining overall charge neutrality of the clusters. This enforces proton transfer processes observed in the lowest free-energy structures. All generated structures were subsequently optimized using the semi-empirical GFN1-xTB method (Grimme et al., 2017). DFT single-point energies were then evaluated at the B97-3c level of theory (Brandenburg et al., 2018) on the GFN1-xTB optimized conformers.

To reduce the number of total conformers, high-energy configurations were removed by retaining only the 1,000 lowest-energy conformers for further refinement. These structures were subjected to partial geometry optimization with $n \times 2$ iterations (n being the number of acid–base pairs) at the B97-3c level to efficiently eliminate energetically unfavorable configurations. From this subset, the 100 most stable structures were selected for full geometry optimization followed by vibrational frequency calculations.

The lowest free energy conformer was then selected for additional CREST exploration as suggested by Knattrup et al. (2024), using the following workflow:

$$\text{CREST} \xrightarrow{N=100} \text{B97-3c}^{\text{FULL OPT}} \qquad \text{(CREST track)}$$

The configurational exploration was then carried out using CREST at the GFN1-xTB/GFN1-xTB$^{\text{re-par}}$ level in the non-covalent interaction mode. Then, the 100 lowest-energy geometries were selected for full optimization, and vibrational frequency calculations.

2.3 Machine learning-enhanced configurational sampling of $(MSA)_1(SA)_{n-1}(AM/MA/DMA)n$, with $n = 6 - 10$ clusters

The PaiNN (Schütt et al., 2021) architecture, as implement in SchNetPack (Schütt et al., 2019, 2023), was used to learn the energy and forces at the B97-3c level of theory. We used the hyperparameters suggested by Kubečka et al. (2024), who found the PaiNN model to performed excellently in reproducing the geometries at the B97-3c level of theory for atmospheric molecular

https://doi.org/10.5194/ar-2026-23
Preprint. Discussion started: 24 June 2026

AEROSOL Research Discussions

clusters. The $(MSA)_1(SA)_{n-1}(AM/MA/DMA)n$ cluster structures with $n = 1$–5 identified in the previous section was used as a training/validation set. A separate model was trained for each base system. The training data consisted of out of equilibrium structures (the initial GFN1-xTB structures with B97-3c single point energies and forces) and equilibrium structures calculated at the B97-3c level. The number of structures were filtered based on gyration radius, electronic energy and dipole moment using arbitrary thresholds until a manageable amount of data was left. This resulted in a training/validation set of 9645, 6746, and 8681 structures for the SA–MSA–AM, SA–MSA–MA, and SA–MSA–DMA models, respectively. The models were trained for 600 epochs which yielded validation errors below 0.012 kcal/mol for all 3 models. Using the trained neural networks, the configurational sampling of the $n = 6 - 10$ clusters was performed as following:

$$\text{ABC} \xrightarrow{N=10{,}000} \text{xTB}^{\text{OPT}} \xrightarrow{N=10{,}000} \text{NN}^{\text{OPT}} \xrightarrow{N=10{,}000} \text{B97-3c}^{\text{SP}} \xrightarrow[\text{filter}]{\text{N=100}} \text{B97-3c}^{\text{FULL OPT}} \qquad \text{(NN track)}$$

where the optimization using the neural network was performed using ASE (Larsen et al., 2017), with the BFGS optimizer, for 600 steps. Although we found the geometries to be reliable and closer to the true B97-3c minimum, a single-point calculation at the B97-3c was needed to get the correct energy order. The 100 lowest electronic energy geometries were selected for full optimization, and vibrational frequency calculations were performed. This was followed by the CREST track workflow.

2.4 Configurational sampling of $(MSA)_n(AM/MA/DMA)_n$, with $n = 1 - 10$ clusters

The pure $(MSA)_n(AM/MA/DMA)_n$ clusters were sampled without machine learning using the full workflow in section 2.2 for the set of clusters with n up to 10.

2.5 Cluster Binding Free Energies

The thermodynamic stability of the clusters was calculated through their standard binding free energies defined as the difference between the Gibbs free energy of the cluster and the sum of the Gibbs free energies of the isolated monomers. The binding free energy is therefore expressed as

$$\Delta G_{\text{bind}} = G_{\text{cluster}} - \sum_i G_{\text{monomer},i}. \qquad (1)$$

Equation (1) above describe the intrinsic thermochemistry of the clusters under standard conditions. The quasi-harmonic approximation, with a 100 cm^{-1}, threshold was employed to calculate the vibrational entropy contribution (Grimme, 2012).

To evaluate effective binding free energies under specific atmospheric conditions, we employ the self-consistent distribution formalism (Wilemski and Wyslouzil, 1995; Halonen, 2022),

$$\Delta G_{\text{bind}}(\boldsymbol{p}) = \Delta G_{\text{bind}} - RT \cdot \left(1 - \frac{1}{n}\right) \cdot \sum_i \ln\left(\frac{p_i}{p_{\text{ref}}}\right). \qquad (2)$$

Here, n denotes the total number of molecules in the cluster, p_{ref} denotes the reference pressure (1 atm) and p_i represents the partial pressure of monomer i. This self-consistent formulation ensures that the reference free energies of the isolated monomers are properly defined as zero under the chosen thermodynamic reference state.

https://doi.org/10.5194/ar-2026-23
Preprint. Discussion started: 24 June 2026

AEROSOL Research Discussions

3 Results and discussion

3.1 Binding free energies under standard conditions

Using the configurational sampling workflow described above, we studied clusters containing SA, MSA, and atmospherically relevant bases, focusing on the $(\mathrm{acid})_n(\mathrm{base})_n$ stoichiometries up to $n = 10$. We studied SA–MSA–AM, SA–MSA–MA, and SA–MSA–DMA clusters, as well as the corresponding limiting case containing only MSA as the acidic component. The SA–base clusters were taken from Wu et al. (2024). The calculated standard binding free energies at 298.15 K and 1 atm are shown as a function of molecules in the cluster m, and each point is labeled according to the acid composition, e.g. (SA, MSA).

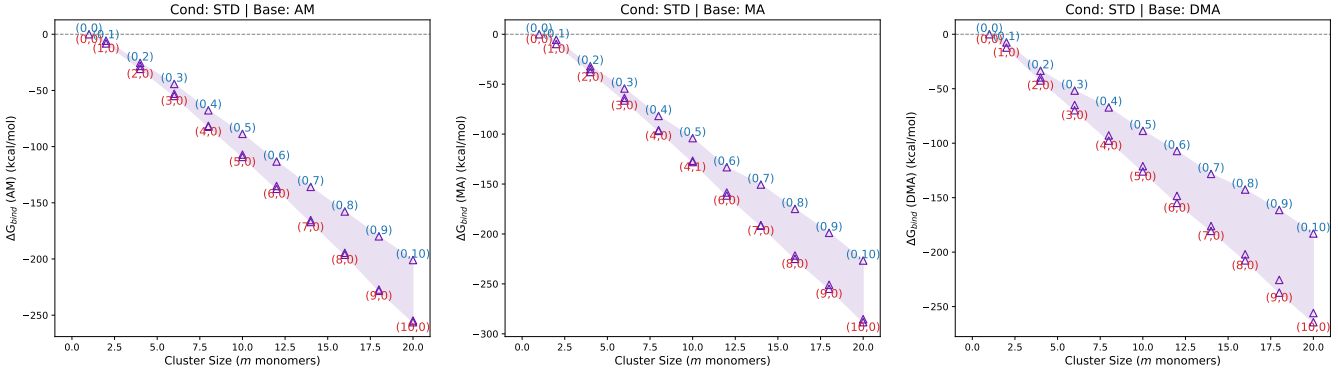

Figure 1. Binding Gibbs free energies (ΔG_{bind}) at the B97-3c level of theory under standard conditions (STD) for clusters containing SA, MSA, and bases (AM, MA, DMA). The shaded region represents the range between minimum and maximum values for each cluster size, while annotations indicate the acid composition (SA, MSA).

Based on the standard binding free energies (**Figure 1**), we observe a clear hierarchy: clusters containing SA are consistently more stable than the corresponding clusters containing only MSA. This trend is observed for all three bases studied here. This is expected chemically, since SA is a considerably stronger acid than MSA and therefore leads to stronger acid–base interactions. As a result, SA-containing clusters are thermodynamically stabilized against evaporation. This trend also persists as cluster size increases. Replacing one SA molecule with MSA does not provide any substantial energetic benefit and, in many cases, leads to less favorable binding free energies. This behavior is particularly pronounced for the DMA-containing systems, where the strong SA–DMA interaction already defines the thermodynamic landscape, leaving little room for MSA to contribute meaningfully to stabilization. Hence, for DMA-containing systems, MSA does not appear to participate in any notable acid synergy at the earliest stages of cluster formation.

A particularly clear example is the DMA system at the largest size studied (20 monomers, i.e. 10 acids + 10 bases): the pure SA–DMA cluster has a binding free energy of roughly $-264\ \mathrm{kcal\,mol^{-1}}$, while the pure MSA–DMA analogue is about $-183\ \mathrm{kcal\,mol^{-1}}$, a difference of $\sim 81\ \mathrm{kcal\,mol^{-1}}$ in favor of SA. The same qualitative pattern holds for AM and MA (e.g., at 20 monomers, MSA-only clusters are $\sim$ 55–62 $\mathrm{kcal\,mol^{-1}}$ less stable than SA-only clusters for AM and MA, respectively).

https://doi.org/10.5194/ar-2026-23
Preprint. Discussion started: 24 June 2026

AEROSOL Research Discussions

We note that this mixed-acid behavior differs markedly from the mixed-base synergy previously observed in SA–AM–DMA systems (Hasan et al., 2025). In those mixed-base systems, the introduction of one or two AM molecules into SA–DMA clusters produced a clear stabilization effect for larger clusters, despite DMA being the intrinsically stronger base. This behavior was attributed to the higher hydrogen-bond coordination capacity of AM, which enabled the formation of more favorable and increasingly particle-like bonding networks as the clusters grew.

In contrast, the present mixed-acid systems do not exhibit a comparable synergistic stabilization upon replacing SA with MSA. Although mixed-acid clusters remain less stable than their pure-SA counterparts, the energetic penalty associated with MSA substitution decreases systematically with increasing cluster size. This trend indicates that the stronger intrinsic acidity of SA dominates the thermodynamics of the smallest clusters, whereas incorporation of MSA becomes progressively more favorable during growth. The effect is particularly evident for the SA–MSA–AM and SA–MSA–MA systems, where the free-energy differences relative to the pure-SA clusters diminish at larger sizes, suggesting a greater role for MSA in later growth stages than in the initial nucleation process.

https://doi.org/10.5194/ar-2026-23
Preprint. Discussion started: 24 June 2026

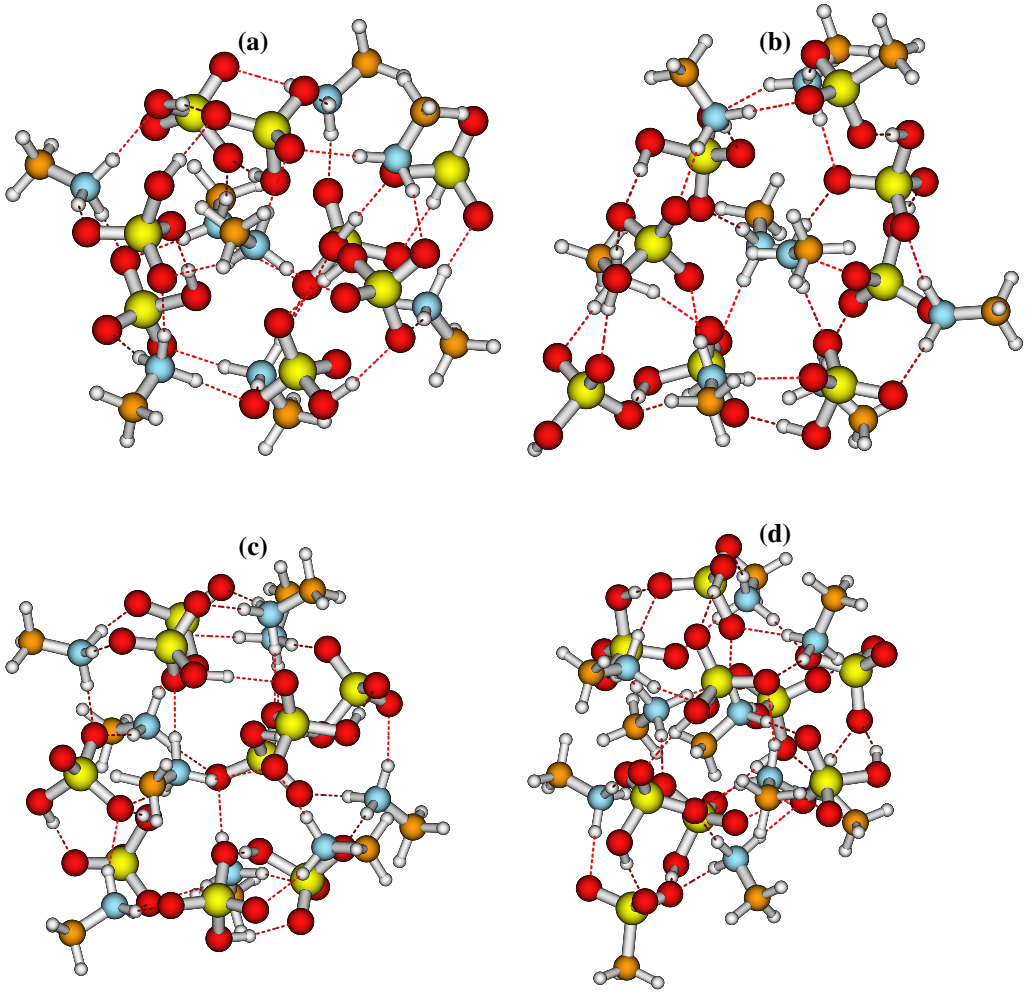

Figure 2. Comparison of pure and mixed-acid clusters for the MA system. (a) $(SA)_8(MA)_8$, (b) $(MSA)_1(SA)_7(MA)_8$, (c) $(SA)_9(MA)_9$, (d) $(MSA)_1(SA)_8(MA)_9$.

This suggests that, although MSA does not enhance stability relative to pure-SA clusters, its incorporation becomes increasingly favorable as cluster size increases. A plausible explanation is that larger clusters possess more extended hydrogen-bonding networks (Figure 2), allowing the methyl-group perturbation to be distributed across the cluster. In contrast, the more compact bonding motifs of smaller clusters are less able to accommodate this perturbation, resulting in a larger energetic penalty for MSA substitution.

Structurally, both the pure-SA and mixed-acid clusters exhibit a gradual transition from relatively compact molecular complexes toward increasingly particle-like three-dimensional hydrogen-bonding networks as cluster size increases. The incorporation of one MSA molecule does not qualitatively alter this cluster-to-particle transition behavior. Instead, the main effect of MSA appears to be a modest perturbation of the hydrogen-bonding arrangement due to the presence of the methyl group, which slightly reduces the hydrogen-bond coordination efficiency compared to SA. This effect may be particularly important in DMA-containing clusters, where the additional methyl groups of DMA already impose steric constraints on the cluster ge-

https://doi.org/10.5194/ar-2026-23
Preprint. Discussion started: 24 June 2026

AEROSOL Research Discussions

ometry. Consequently, simultaneous incorporation of both DMA and MSA may further reduce the ability of the cluster to form compact and efficiently coordinated hydrogen-bonding motifs.

Overall, the standard free energy data indicate that MSA is not a strong nucleating acid on its own, and SA remains the dominant acid controlling the thermodynamics of initial cluster formation. However, MSA could potentially incorporate into the cluster at larger sizes, thus contributing to the cluster growth. In general, the contribution of MSA to cluster stabilization is highly dependent on both cluster size and base type.

3.2 Binding free energies under given conditions

Based on the calculated standard binding free energies described above, we recalculated the binding free energies under atmospherically relevant monomer concentrations and temperatures using equation (2). Figures 3–6 present the binding Gibbs free energies of the mixed-acid clusters at 278.15 and 298.15 K under four representative concentration regimes. These include high-concentration conditions at 278.15 K ($[\mathrm{SA}] = [\mathrm{MSA}] = 10^8$ molec. cm^{-3}; denoted 278H), high-MSA conditions at 278.15 K ($[\mathrm{SA}] = 10^6$ and $[\mathrm{MSA}] = 10^8$ molec. cm^{-3}; denoted 278Hmsa), low-concentration conditions at 298.15 K ($[\mathrm{SA}] = [\mathrm{MSA}] = 10^6$ molec. cm^{-3}; denoted 298L), and high-MSA conditions at 298.15 K ($[\mathrm{SA}] = 10^6$ and $[\mathrm{MSA}] = 10^8$ molec. cm^{-3}; denoted 298Hmsa).

In all cases, the base concentrations were fixed at AM = 10 ppb and amines (MA, DMA) = 5 ppt. These conditions were chosen to mimic typical chamber and atmospheric environments, and to assess how the relative abundance of SA and MSA influences the stability and composition of the earliest clusters. In the following, we discuss each scenario separately.

3.2.1 Low SA–low MSA concentrations at 298.15 K

Under low-concentration conditions at 298.15 K, the calculated free energies (**Figure 3**) show that clusters containing SA remain clearly favored over those dominated by MSA. This trend is particularly strong for the DMA-containing system, where the SA–MSA–DMA clusters essentially show no energetic advantage from incorporating MSA. The lowest-free-energy clusters remain those with the highest SA content, demonstrating that MSA does not compete effectively with SA when paired with a strong base such as DMA.

https://doi.org/10.5194/ar-2026-23
Preprint. Discussion started: 24 June 2026

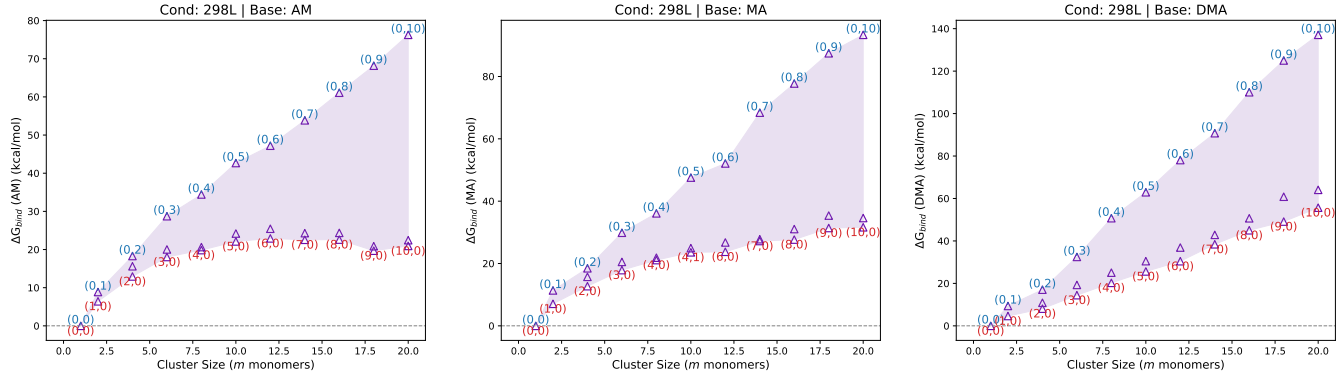

Figure 3. Binding Gibbs free energies (ΔG_{bind}) at the B97-3c level of theory at 298.15 K under low concentration conditions (298L), with $[\mathrm{SA}] = [\mathrm{MSA}] = 10^6$ molec. cm^{-3}. Base concentrations are fixed at AM = 10 ppb and amines (MA, DMA) = 5 ppt.

The AM- and MA-containing systems are somewhat more sensitive to acid composition; however, even in these cases, the pure or SA-rich clusters remain lowest in free energy at the smallest sizes. Thus, under warm and dilute conditions, MSA does not appear capable of driving the initial formation of stable clusters. Instead, it behaves as a weaker auxiliary acid that may only enter the cluster after SA has already established the primary acid–base scaffold. Hence, at such conditions, it is expected that MSA only affect the growth of FNPs. Overall, at ambient conditions and low concentration of the acids, the thermodynamic landscape is uphill and thereby it is unlikely that FNP formation will occur.

This result has important implications for previous experimental observations (Perraud et al., 2020; Chen et al., 2015) reporting efficient particle formation in MSA–MA systems. The present calculations suggest that binary MSA–base interactions alone are unlikely to fully explain the experimentally observed particle formation efficiencies. In particular, our simulations do not include additional stabilizing species such as water molecules or ions, which are commonly present under experimental and atmospheric conditions and are known to substantially enhance cluster stability and suppress evaporation. Indeed, previous experimental studies have also highlighted the important role of water in promoting particle formation in MSA-containing systems (Perraud et al., 2020; Chen et al., 2015). Therefore, the discrepancy between the our calculations and experimentally observed particle formation rates is likely related to the simplified dry-cluster framework employed here rather than an inconsistency with the experimental observations themselves.

3.2.2 High MSA–Low SA concentrations at 298.15 K

At 298.15 K and higher MSA concentrations, the overall cluster free energies (**Figure 4**) become less positive. Under these conditions, the differences between cluster compositions narrow somewhat, and mixed-acid clusters become more competitive in the AM- and MA-containing systems.

https://doi.org/10.5194/ar-2026-23
Preprint. Discussion started: 24 June 2026

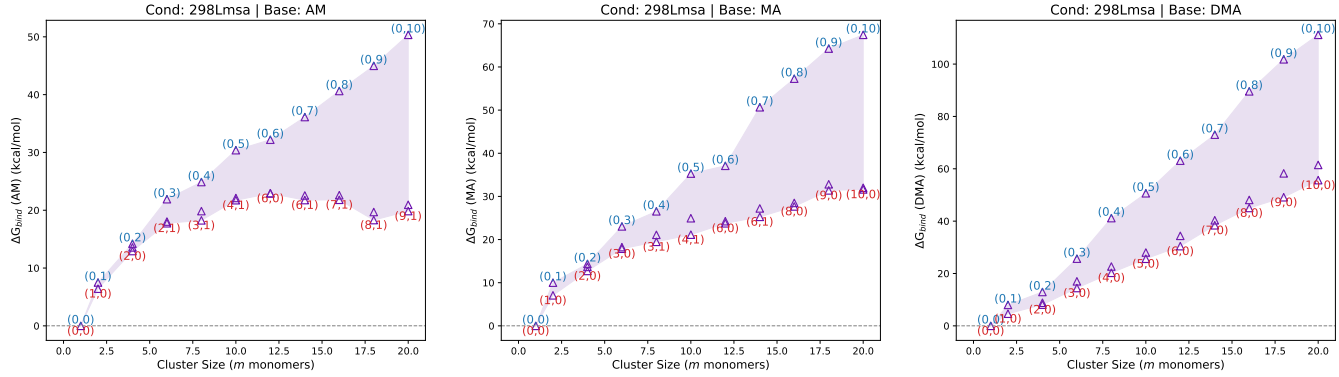

Figure 4. Binding Gibbs free energies (ΔG_{bind}) at the B97-3c level of theory at 298.15 K under low SA and high MSA concentration conditions (298Hmsa), with $[\mathrm{SA}] = 10^6$ and $[\mathrm{MSA}] = 10^8$ molec. cm^{-3}. Base concentrations are fixed at AM = 10 ppb and amines (MA, DMA) = 5 ppt.

In particular, the SA–MSA–AM and SA–MSA–MA clusters show that MSA can begin to contribute to cluster stabilization when its relative abundance is sufficiently high. For instance, for SA–MSA–AM we see clusters containing one MSA being most stable across almost all size ranges. This does not change the overall conclusion that SA remains the dominant nucleating acid, but it suggests that MSA can influence the growth trajectory once the cluster has reached a sufficient size. Although this effect remains clearly weaker than that of SA, it indicates that MSA may become incorporated into growing clusters under favorable concentration conditions.

For the SA–MSA–DMA system, however, the conclusions remain unchanged. Even at elevated MSA concentrations, the strong SA–DMA interaction dominates the cluster energetics, and MSA contributes little to the stabilization. Thus, the presence of a strong base suppresses any meaningful acid synergy between SA and MSA. Overall, we see now role of MSA in cluster formation at 298.15 K, despite having a 100 times higher concentration than SA. However, the overall conclusion is similar to the Low SA–low MSA concentrations, at 298.15 K, i.e. it is unlikely that FNP formation will occur at these conditions.

3.2.3 High MSA–Low SA concentrations at 278.15 K

At 278.15 K and high concentrations of MSA, the free-energy surfaces (**Figure 5**) become increasingly downhill for the larger clusters containing AM and MA, indicating more favorable growth conditions under these low temperature and high concentrations of MSA. Nevertheless, both systems still exhibit an initial nucleation barrier at the smallest cluster sizes before growth becomes thermodynamically favorable. In contrast, the DMA-containing cluster remain strongly stabilized primarily by SA, while the pure MSA–DMA clusters remain purely uphill despite the enhanced MSA concentration.

https://doi.org/10.5194/ar-2026-23
Preprint. Discussion started: 24 June 2026

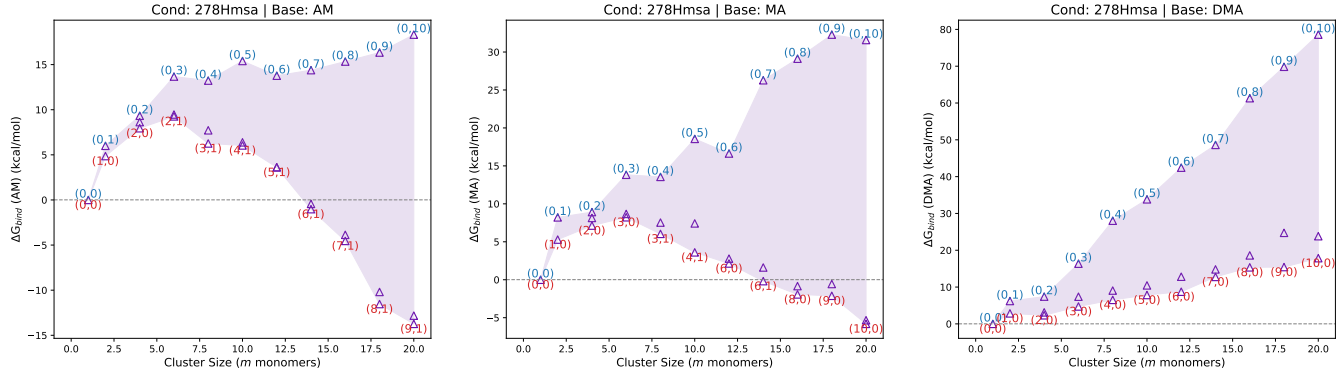

Figure 5. Binding Gibbs free energies (ΔG_{bind}) at the B97-3c level of theory at 278.15 K under high MSA concentration conditions (278Hmsa), with $[\mathrm{SA}] = 10^6$ and $[\mathrm{MSA}] = 10^8$ molec. cm^{-3}. Base concentrations are fixed at AM = 10 ppb and amines (MA, DMA) = 5 ppt.

Under these conditions, the AM- and MA-containing mixed-acid systems again show the greatest sensitivity to MSA incorporation. In these systems, MSA can contribute to cluster stabilization at intermediate and larger sizes, especially when SA is not overwhelmingly dominant in the gas phase. However, even under the most favorable conditions for MSA participation, the calculations do not support a scenario in which MSA replaces SA as the primary nucleating acid. Instead, MSA acts as a secondary growth-modifying species, entering the cluster once the main SA-driven acid–base clusters are established. In the SA–MSA–DMA system, the strong SA–DMA pair continues to dominate the thermodynamics, and MSA again contributes negligibly. Thus, even when both low temperature and high concentration favor clustering, MSA cannot compete with sulfuric acid in the presence of the strongest base.

3.2.4 High MSA– high SA concentrations at 278.15 K

At the lower temperature of 278.15 K and high concentrations (**Figure 6**), all clusters become more stable compared to the corresponding 298.15 K case. Nevertheless, SA-containing clusters are still significantly favored over MSA-only clusters, confirming that the intrinsic weakness of MSA relative to SA is not compensated simply by lowering the temperature.

https://doi.org/10.5194/ar-2026-23
Preprint. Discussion started: 24 June 2026

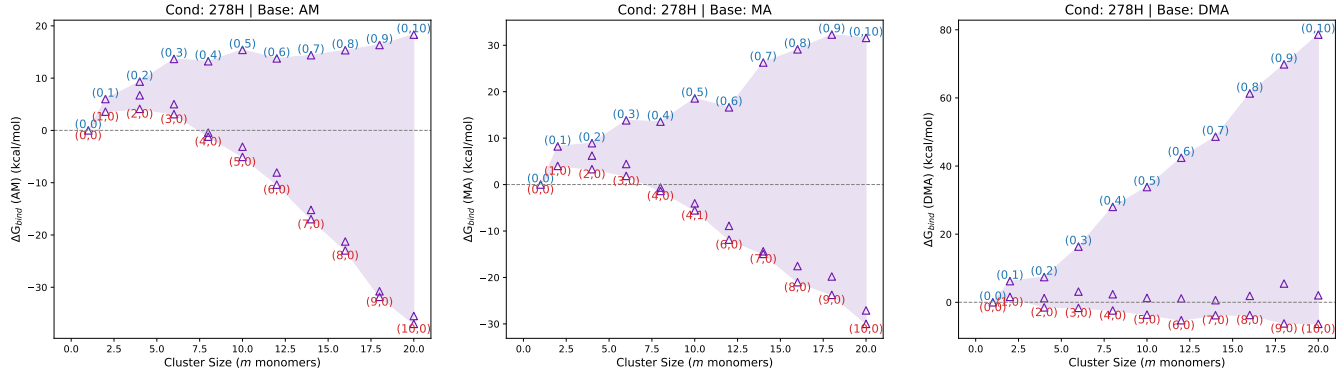

Figure 6. Binding Gibbs free energies (ΔG_{bind}) at the B97-3c level of theory at 278.15 K under high concentration conditions (278H), with $[\mathrm{SA}] = [\mathrm{MSA}] = 10^8$ molec. cm^{-3}. Base concentrations are fixed at AM = 10 ppb and amines (MA, DMA) = 5 ppt.

The SA–MSA–AM and SA–MSA–MA systems again exhibit compositions in which MSA becomes more competitive at larger cluster sizes, indicating a possible role during the early growth stages. Under these conditions, the free-energy barriers for the AM- and MA-containing systems are also go downhill after the initial dimer cluster is formed compared to the warmer conditions, suggesting that particle formation may become thermodynamically more favorable. Nevertheless, the smallest thermodynamically viable clusters remain predominantly SA-dominated.

For the SA–MSA–DMA systems, the strong SA–DMA interaction continues to dominate the thermodynamics, and the corresponding free-energy surfaces become nearly fully downhill under these conditions. In contrast, the pure MSA-containing DMA clusters remain significantly less favorable, indicating that MSA still contributes only weakly to the stabilization pattern in the presence of DMA.

Overall, these results suggest that, although lowering the temperature enhances clustering and reduces nucleation barriers in general, the relative importance of MSA is governed more strongly by composition and concentration than by temperature alone. Thus, even under favorable low-temperature and high-MSA conditions, SA remains the key acid controlling the earliest nucleation steps.

3.2.5 Low temperature and MSA-rich conditions at 258.15 K

Finally, we tested an additional condition at a relatively low temperature of 258.15 K with an SA:MSA ratio of 1:1000. Under low temperature conditions at 258.15 K with a strong excess of MSA relative to SA (**Figure 7**), the stability of MSA-containing clusters increases substantially compared to warmer conditions. In particular, the pure MSA-containing systems become significantly more competitive at larger cluster sizes, indicating that low temperature combined with high MSA abundance can enhance the thermodynamic contribution of MSA to cluster growth.

https://doi.org/10.5194/ar-2026-23
Preprint. Discussion started: 24 June 2026

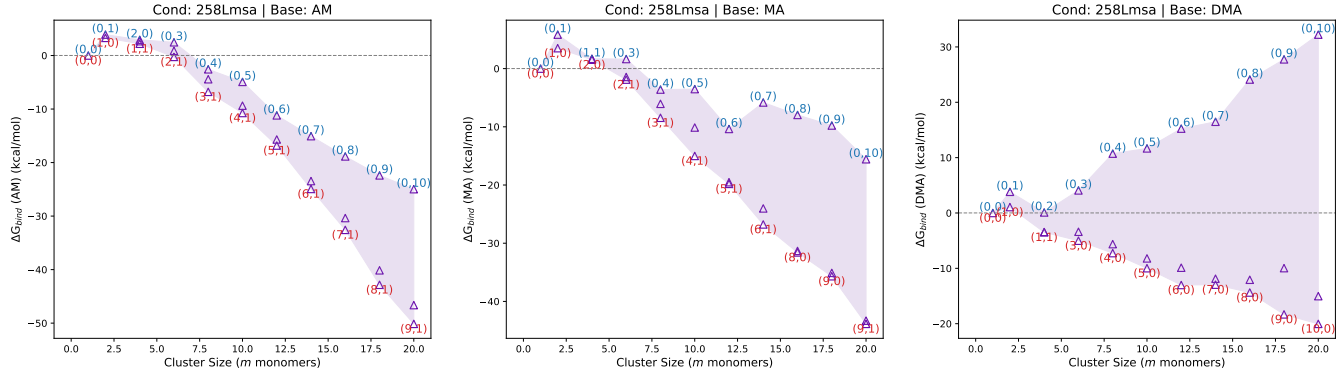

Figure 7. Binding Gibbs free energies (ΔG_{bind}) at the B97-3c level of theory at 258.15 K under MSA-rich conditions (258Lmsa), with $[\mathrm{SA}] = 10^6$ and $[\mathrm{MSA}] = 10^9$ molec.,cm^{-3}. Base concentrations are fixed at AM = 10 ppb and amines (MA, DMA) = 5 ppt.

The effect is most pronounced for the DMA-containing clusters, where the free energies of the pure MSA systems decrease considerably relative to the corresponding higher-temperature cases. Nevertheless, even under these highly MSA-favored conditions, mixed SA-containing clusters generally remain among the most stable configurations, particularly at smaller cluster sizes. The SA–MSA–AM and SA–MSA–MA systems also exhibit enhanced stabilization from MSA incorporation at larger sizes, suggesting that MSA may become increasingly relevant during the cluster growth regime.

Overall, while SA-containing clusters still dominate the earliest nucleation steps, these results indicate that the thermodynamic importance of MSA increases strongly under cold and MSA-rich atmospheric conditions. This is consistent with the previous work by Rasmussen et al. (2022). The formation of MSA from the oxidation of DMS by OH radicals has been shown to be temperature dependent (Barnes et al., 2006; Shen et al., 2022). Hence, under colder conditions, the MSA:SA ratio will be high, due to a shift from the hydrogen abstraction pathway to the OH radical addition pathway. This indicates that MSA might contribute to the early growth of FNPs, but is still unlikely to participate in the very initial particle formation steps, when SA and DMA are present.

4 Conclusions

Here, we find that the acid synergy between SA and MSA is qualitatively different and significantly weaker than the mixed-base synergy previously observed for SA–AM–DMA clusters. In the mixed-base case, combining strong and weak bases showed clear synergistic stabilization effects in larger clusters, whereas the present mixed-acid systems remain dominated by the intrinsically stronger acidity of SA relative to MSA.

Overall, the calculations show that pure MSA-containing acid–base clusters are generally not sufficiently stable to drive efficient initial nucleation under most atmospherically relevant conditions investigated here. Instead, SA-containing clusters consistently dominate the earliest cluster formation steps, particularly in systems involving DMA, where the strong SA–DMA interaction leads to nearly barrierless cluster growth under favorable conditions. In contrast, the AM- and MA-containing

https://doi.org/10.5194/ar-2026-23
Preprint. Discussion started: 24 June 2026

systems exhibit larger nucleation barriers, although these barriers decrease substantially at lower temperatures and elevated MSA concentrations.

The calculations further indicate that MSA contributes primarily during the early growth regime rather than the initial nucleation step itself. In particular, MSA incorporation becomes increasingly favorable at larger cluster sizes, especially in SA–MSA–AM and SA–MSA–MA systems under conditions of low temperature and elevated MSA:SA ratios. Under the most MSA-rich and coldest conditions considered here (258.15 K and SA:MSA = 1:1000), the thermodynamic stability of MSA-containing clusters increases substantially, and the free-energy penalties associated with MSA incorporation decrease remarkably. Nevertheless, even under these strongly MSA-favored conditions, SA-containing clusters remain among the most stable structures at the smallest cluster sizes.

From an atmospheric perspective, these findings suggest that the role of MSA in particle formation depends strongly on environmental conditions. Over marine environments and colder atmospheric regions, where dimethyl sulfide oxidation may favor MSA formation relative to SA, MSA could become increasingly important for stabilizing growing clusters and enhancing early particle growth. However, our results suggest that substantially lower temperatures and/or even more extreme MSA:SA ratios than those considered here would likely be required for pure MSA-driven clustering to become fully downhill and competitive with SA-driven nucleation.

Finally, it is important to emphasize that this study does not include additional stabilizing species such as water molecules or ions. Previous experimental studies have highlighted the important role of water in promoting particle formation in MSA-containing systems, and inclusion of water may substantially reduce evaporation rates and enhance cluster stability. Thus, while the present work isolates the intrinsic thermodynamic role of MSA in mixed-acid clustering, future studies including hydration and ionic effects will be necessary for a more complete description of atmospheric particle formation under realistic marine conditions.

Data availability. All the calculated structures and thermochemistry are available in the Atmospheric Cluster Database (ACDB) at: https://github.com/elmjonas/ACDB/tree/master/Articles/

Author contributions. Conceptualization: J.E.;
Methodology: G.H., Y.K., H.W., J.E.;
Formal analysis: G.H., Y.K., H.W.;
Investigation: G.H., Y.K., H.W.;
Resources: J.E.;
Writing - original draft: G.H.;
Writing - review & editing: G.H., Y.K., H.W., J.E.;
Visualization: G.H, H.W.;
Project administration: J.E.;

https://doi.org/10.5194/ar-2026-23
Preprint. Discussion started: 24 June 2026

Funding acquisition: J.E;
Supervision: J.E.

Competing interests. J.E is a member of the Editorial Board of Aerosol Research. The remaining authors have no conflict of interests to declare.

Disclaimer. Funded by the European Union. Views and opinions expressed are however those of the authors only and do not necessarily reflect those of the European Union, the European Research Executive Agency, or the European Research Council Executive Agency. Neither the European Union nor the granting authority can be held responsible for them.

Acknowledgements. This work was funded by the European Union (ERC, ExploreFNP, project 101040353) and the Danish National Research Foundation (DNRF172) through the Center of Excellence for Chemistry of Clouds.

The numerical results presented in this work were obtained at the Centre for Scientific Computing, Aarhus https://phys.au.dk/forskning/faciliteter/cscaa/.

https://doi.org/10.5194/ar-2026-23
Preprint. Discussion started: 24 June 2026

References

Alfaouri, D., Passananti, M., Zanca, T., Ahonen, L., Kangasluoma, J., Kubečka, J., Myllys, N., and Vehkam"aki, H.: A Study on the Fragmentation of Sulfuric Acid and Dimethylamine Clusters Inside an Atmospheric Pressure Interface Time-of-Flight Mass Spectrometer, Atmos. Meas. Tech., 15, 11–19, 2022.

Almeida, J., Schobesberger, S., K"urten, A., Ortega, I. K., Kupiainen-M"a"att"a, O., Praplan, A. P., Adamov, A., Amorim, A., Bianchi, F., Breitenlechner, M., and et al.: Molecular Understanding of Sulphuric Acid–Amine Particle Nucleation in the Atmosphere, Nature, 502, 359–363, 2013.

Bannwarth, C., Caldeweyher, E., Ehlert, S., Hansen, A., Pracht, P., Seibert, J., Spicher, S., and Grimme, S.: Extended Tight-Binding Quantum Chemistry Methods, WIREs Comput. Mol. Sci., 11, e1493, https://doi.org/10.1002/wcms.1493, 2021.

Barnes, I., Hjorth, J., and Mihalopoulos, N.: Dimethyl Sulfide and Dimethyl Sulfoxide and Their Oxidation in the Atmosphere, Chem. Rev., 106, 940–975, 2006.

Bates, T., Lamb, B., Guenther, A., Dignon, J., and Stoiber, R.: Sulfur Emissions to the Atmosphere from Natural Sources, J. Atmos. Chem., 14, 315–337, 1992.

Bianchi, F., Tr"ostl, J., Junninen, H., Frege, C., Henne, S., Hoyle, C. R., Molteni, U., Herrmann, E., Adamov, A., Bukowiecki, N., et al.: New Particle Formation in the Free Troposphere: A Question of Chemistry and Timing, Science, 352, 1109–1112, 2016.

Brandenburg, J. G., Bannwarth, C., Hansen, A., and Grimme, S.: B97-3c: A Revised Low-Cost Variant of the B97-D Density Functional Method, J. Chem. Phys., 148, 064 104, https://doi.org/10.1063/1.5012601, 2018.

Chen, H., Ezell, M. J., Arquero, K. D., Varner, M. E., Dawson, M. L., Gerber, R. B., and Finlayson-Pitts, B. J.: New Particle Formation and Growth from Methanesulfonic Acid, Trimethylamine and Water, Phys. Chem. Chem. Phys., 17, 13 699–13 709, 2015.

Cooley, S., Schoeman, D., Bopp, L., Boyd, P., Donner, S., Kiessling, W., Martinetto, P., Ojea, E., Racault, M., Rost, B., et al.: Oceans and Coastal Ecosystems and Their Services, 2023.

Cromar, K. and Lazrak, N.: Risk Communication of Ambient Air Pollution in the WHO European Region: Review of Air Quality Indexes and Lessons Learned, 2023.

DePalma, J. W., Bzdek, B. R., Doren, D. J., and Johnston, M. V.: Structure and Energetics of Nanometer-Size Clusters of Sulfuric Acid with Ammonia and Dimethylamine, J. Phys. Chem. A, 116, 1030–1040, 2012.

DePalma, J. W., Doren, D. J., and Johnston, M. V.: Formation and Growth of Molecular Clusters Containing Sulfuric Acid, Water, Ammonia, and Dimethylamine, J. Phys. Chem. A, 118, 5464–5473, 2014.

Eisele, F. and Tanner, D.: Measurement of the Gas-Phase Concentration of H2SO4 and Methane Sulfonic Acid and Estimates of H2SO4 Production and Loss in the Atmosphere, J. Geophys. Res. Atmos., 98, 9001–9010, 1993.

Facchini, M. C., Decesari, S., Rinaldi, M., Carbone, C., Finessi, E., Mircea, M., Fuzzi, S., Moretti, F., Tagliavini, E., Ceburnis, D., et al.: Important Source of Marine Secondary Organic Aerosol from Biogenic Amines, Environ. Sci. Technol., 42, 9116–9121, 2008.

Ge, X., Wexler, A. S., and Clegg, S. L.: Atmospheric Amines–Part I. A Review, Atmos. Environ., 45, 524–546, 2011.

Grimme, S.: Supramolecular Binding Thermodynamics by Dispersion-Corrected Density Functional Theory, Chem. Eur. J, 18, 9955–9964, 2012.

Grimme, S.: Exploration of Chemical Compound, Conformer, and Reaction Space with Meta-Dynamics Simulations Based on Tight-Binding Quantum Chemical Calculations, J. Chem. Theory Comput., 15, 2847–2862, 2019.

https://doi.org/10.5194/ar-2026-23
Preprint. Discussion started: 24 June 2026

Grimme, S., Bannwarth, C., and Shushkov, P.: A Robust and Accurate Tight-Binding Quantum Chemical Method for Structures, Vibrational Frequencies, and Noncovalent Interactions of Large Molecular Systems Parametrized for All spd-Block Elements (Z = 1–86), J. Chem. Theory Comput., 13, 1989–2009, 2017.

Halonen, R.: A Consistent Formation Free Energy Definition for Multicomponent Clusters in Quantum Thermochemistry, J. Aerosol Sci., 162, 105 974, 2022.

Hasan, G., Wu, H., Knattrup, Y., and Elm, J.: Base Synergy in Freshly Nucleated Particles, Aerosol Res., 3, 101–111, 2025.

Henschel, H., Navarro, J. C. A., Yli-Juuti, T., Kupiainen-M"a"att"a, O., Olenius, T., Ortega, I. K., Clegg, S. L., Kurt'en, T., Riipinen, I., and Vehkam"aki, H.: Hydration of Atmospherically Relevant Molecular Clusters: Computational Chemistry and Classical Thermodynamics, J. Phys. Chem. A, 118, 2599–2611, 2014.

Henschel, H., Kurt'en, T., and Vehkam"aki, H.: Computational Study on the Effect of Hydration on New Particle Formation in the Sulfuric Acid/Ammonia and Sulfuric Acid/Dimethylamine Systems, J. Phys. Chem. A, 120, 1886–1896, 2016.

Herb, J., Nadykto, A. B., and Yu, F.: Large Ternary Hydrogen-Bonded Pre-Nucleation Clusters in the Earth's Atmosphere, Chem. Phys. Lett., 518, 7–14, 2011.

Huang, J. and MacKerell Jr, A. D.: CHARMM36 All-Atom Additive Protein Force Field: Validation Based on Comparison to NMR Data, J. Comput. Chem., 34, 2135–2145, 2013.

Ianni, J. C. and Bandy, A. R.: A Density Functional Theory Study of the Hydrates of $NH_3 \cdot H_2SO_4$ and Its Implications for the Formation of New Atmospheric Particles, J. Phys. Chem. A, 103, 2801–2811, 1999.

Jokinen, T., Sipil"a, M., Junninen, H., Ehn, M., L"onn, G., Hakala, J., Pet"aj"a, T., Mauldin III, R., Kulmala, M., and Worsnop, D.: Atmospheric Sulphuric Acid and Neutral Cluster Measurements Using CI-APi-TOF, Atmos. Chem. Phys., 12, 4117–4125, 2012.

Kirkby, J., Curtius, J., Almeida, J., Dunne, E., Duplissy, J., Ehrhart, S., Franchin, A., Gagn'e, S., Ickes, L., K"urten, A., et al.: Role of Sulphuric Acid, Ammonia and Galactic Cosmic Rays in Atmospheric Aerosol Nucleation, Nature, 476, 429–433, 2011a.

Kirkby, J., Curtius, J., Almeida, J., Dunne, E., Duplissy, J., Ehrhart, S., Franchin, A., Gagne, S., Ickes, L., Kürten, A., Kupc, A., Metzger, A., Riccobono, F., Rondo, L., Schobesberger, S., Tsagkogeorgas, G., Wimmer, D., Amorim, A., Bianchi, F., Breitenlechner, M., David, A., Dommen, J., Downard, A., Ehn, M., Flagan, R., Haider, S., Hansel, A., Hauser, D., Jud, W., Junninen, H., Kreissl, F., Kvashin, A., Laaksonen, A., Lehtipalo, K., Lima, J., Lovejoy, E., Makhmutov, V., Mathot, S., Mikkilä, J., Minginette, P., Mogo, S., Nieminen, T., Onnela, A., Pereira, P., Petäjä, T., Schnitzhofer, R., Seinfeld, J., Sipilää, M., Stozhkov, Y., Stratmann, F., Tomé, A., Vanhanen, J., Viisanen, Y., Vrtala, A., Wagner, P., Walther, H., Weingartner, E., Wex, H., Winkler, P., Carslaw, K., Worsnop, D., Baltensperger, U., and Kulmala, M.: Role of Sulphuric Acid, Ammonia and Galactic Cosmic Rays in Atmospheric Aerosol Nucleation, Nature, 476, 429 – 433, 2011b.

Kirkby, J., Duplissy, J., Sengupta, K., Frege, C., Gordon, H., Williamson, C., Heinritzi, M., Simon, M., Yan, C., Almeida, J., et al.: Ion-Induced Nucleation of Pure Biogenic Particles, Nature, 533, 521–526, 2016.

Knattrup, Y., Kubečka, J., Wu, H., Jensen, F., and Elm, J.: Reparameterization of GFN1-xTB for Atmospheric Molecular Clusters: Applications to Multi-Acid–Multi-Base Systems, RSC Adv., 14, 20 048–20 055, https://doi.org/10.1039/D4RA03021D, 2024.

Kubečka, J., Ayoubi, D., Tang, Z., Knattrup, Y., Engsvang, M., Wu, H., and Elm, J.: Accurate Modeling of the Potential Energy Surface of Atmospheric Molecular Clusters Boosted by Neural Networks, Environ. Sci. Adv., 3, 1438–1451, https://doi.org/10.1039/D4VA00255E, 2024.

Kulmala, M., Kontkanen, J., Junninen, H., Lehtipalo, K., Manninen, H. E., Nieminen, T., Pet"aj"a, T., Sipil"a, M., Schobesberger, S., Rantala, P., et al.: Direct Observations of Atmospheric Aerosol Nucleation, Science, 339, 943–946, 2013.

https://doi.org/10.5194/ar-2026-23
Preprint. Discussion started: 24 June 2026

Kupiainen-Mä"attä, O., Ortega, I. K., Kurt'en, T., and Vehkam"aki, H.: Amine Substitution into Sulfuric Acid–Ammonia Clusters, Atmos. Chem. Phys., 12, 3591–3599, 2012.

Kurt'en, T., Torpo, L., Sundberg, M. R., Kerminen, V., Vehkam"aki, H., and Kulmala, M.: Estimating the NH_3:H_2SO_4 Ratio of Nucleating Clusters in Atmospheric Conditions Using Quantum Chemical Methods, Atmos. Chem. Phys., 7, 2765–2773, 2007.

Kurtén, T., Loukonen, V., Vehkamäki, H., and Kulmala, M.: Amines are Likely to Enhance Neutral and Ion-induced Sulfuric Acid-water Nucleation in the Atmosphere More Effectively than Ammonia, Atmos. Chem. Phys., 8, 4095–4103, 2008.

Larsen, A. H., Mortensen, J. J., Blomqvist, J., Castelli, I. E., Christensen, R., Dułak, M., Friis, J., Groves, M. N., Hammer, B., Hargus, C., Hermes, E. D., Jennings, P. C., Jensen, P. B., Kermode, J., Kitchin, J. R., Kolsbjerg, E. L., Kubal, J., Kaasbjerg, K., Lysgaard, S., Maronsson, J. B., Maxson, T., Olsen, T., Pastewka, L., Peterson, A., Rostgaard, C., Schiøtz, J., Schütt, O., Strange, M., Thygesen, K. S., Vegge, T., Vilhelmsen, L., Walter, M., Zeng, Z., and Jacobsen, K. W.: The atomic simulation environment—a Python library for working with atoms, Journal of Physics: Condensed Matter, 29, 273 002, 2017.

Larson, L. J., Largent, A., and Tao, M.: Structure of the Sulfuric Acid–Ammonia System and the Effect of Water Molecules in the Gas Phase, J. Phys. Chem. A, 103, 6786–6792, 1999.

Liu, Y., Xie, H.-B., Ma, F., Chen, J., and Elm, J.: Amine-Enhanced Methanesulfonic Acid-Driven Nucleation: Predictive Model and Cluster Formation Mechanism, Environ. Sci. Technol., 56, 7751–7760, 2022.

Loeb, N. G. and Kato, S.: Top-of-Atmosphere Direct Radiative Effect of Aerosols over the Tropical Oceans from the Clouds and the Earth's Radiant Energy System (CERES) Satellite Instrument, J. Climate, 15, 1474–1484, 2002.

Loukonen, V., Kurt'en, T., Ortega, I. K., Vehkam"aki, H., P'adua, A. A. H., Sellegri, K., and Kulmala, M.: Enhancing Effect of Dimethylamine in Sulfuric Acid Nucleation in the Presence of Water–A Computational Study, Atmos. Chem. Phys., 10, 4961–4974, 2010.

Ma, Y., Chen, J., Jiang, S., Liu, Y., Huang, T., Miao, S., Wang, C., and Huang, W.: Characterization of the Nucleation Precursor (H_2SO_4-$(CH_3)_2NH$) Complex: Intra-Cluster Interactions and Atmospheric Relevance, RSC Adv., 6, 5824–5836, 2016.

McMurry, P. H.: The History of Condensation Nucleus Counters, Aerosol Sci. Technol., 33, 297–322, 2000.

Meinardi, S., Simpson, I. J., Blake, N. J., Blake, D. R., and Rowland, F. S.: Dimethyl Disulfide (DMDS) and Dimethyl Sulfide (DMS) Emissions from Biomass Burning in Australia, Geophys. Res. Lett., 30, 2003.

Nadykto, A. B. and Yu, F.: Strong Hydrogen Bonding Between Atmospheric Nucleation Precursors and Common Organics, Chem. Phys. Lett., 435, 14–18, 2007.

Nadykto, A. B., Yu, F., Jakovleva, M. V., Herb, J., and Xu, Y.: Amines in the Earth's Atmosphere: A Density Functional Theory Study of the Thermochemistry of Pre-Nucleation Clusters, Entropy, 13, 554–569, 2011.

Nadykto, A. B., Herb, J., Yu, F., and Xu, Y.: Enhancement in the Production of Nucleating Clusters Due to Dimethylamine and Large Uncertainties in the Thermochemistry of Amine-Enhanced Nucleation, Chem. Phys. Lett., 609, 42–49, 2014a.

Nadykto, A. B., Herb, J., Yu, F., and Xu, Y.: Enhancement in the Production of Nucleating Clusters Due to Dimethylamine and Large Uncertainties in the Thermochemistry of Amine-Enhanced Nucleation, Chem. Phys. Lett., 609, 42–49, 2014b.

Nadykto, A. B., Herb, J., Yu, F., Xu, Y., and Nazarenko, E. S.: Estimating the Lower Limit of the Impact of Amines on Nucleation in the Earth's Atmosphere, Entropy, 17, 2764–2780, 2015.

Napari, I., Kulmala, M., and Vehkam"aki, H.: Ternary Nucleation of Inorganic Acids, Ammonia, and Water, J. Chem. Phys., 117, 8418–8425, 2002.

Neese, F.: Software update: The ORCA program system—Version 5.0, WIREs Comput. Mol. Sci., 12, e1606, 2022.

https://doi.org/10.5194/ar-2026-23
Preprint. Discussion started: 24 June 2026

Olenius, T., Kupiainen-M"a"att"a, O., Ortega, I. K., Kurt'en, T., and Vehkam"aki, H.: Free Energy Barrier in the Growth of Sulfuric Acid–Ammonia and Sulfuric Acid–Dimethylamine Clusters, J. Chem. Phys., 139, 084 312, 2013.

Ortega, I. K., Kupiainen-M"a"att"a, O., Kurt'en, T., Olenius, T., Wilkman, O., McGrath, M. J., Loukonen, V., and Vehkam"aki, H.: From Quantum Chemical Formation Free Energies to Evaporation Rates, Atmos. Chem. Phys., 12, 225–235, 2012.

Passananti, M., Zapadinsky, E., Zanca, T., Kangasluoma, J., Myllys, N., Rissanen, M. P., Kurt'en, T., Ehn, M., Attoui, M., and Vehkam"aki, H.: How Well Can We Predict Cluster Fragmentation Inside a Mass Spectrometer?, Chem. Commun., 55, 5946–5949, 2019.

Pelucchi, C., Negri, E., Gallus, S., Boffetta, P., Tramacere, I., and La Vecchia, C.: Long-Term Particulate Matter Exposure and Mortality: A Review of European Epidemiological Studies, BMC Public Health, 9, 453, 2009.

Perraud, V., Xu, J., Gerber, R. B., and Finlayson-Pitts, B.: Integrated Experimental and Theoretical Approach to Probe the Synergistic Effect of Ammonia in Methanesulfonic Acid Reactions with Small Alkylamines, Environ. Sci.: Processes Impacts, 22, 305–328, 2020.

Pracht, P. and Grimme, S.: Calculation of Absolute Molecular Entropies and Heat Capacities Made Simple, Chem. Sci., 12, 6551–6568, 2021.

Pracht, P., Bauer, C. A., and Grimme, S.: Automated and Efficient Quantum Chemical Determination and Energetic Ranking of Molecular Protonation Sites, J. Comput. Chem., 38, 2618–2631, 2017.

Pracht, P., Bohle, F., and Grimme, S.: Automated Exploration of the Low-Energy Chemical Space with Fast Quantum Chemical Methods, Phys. Chem. Chem. Phys., 22, 7169–7192, 2020.

Rasmussen, F. R., Kubečka, J., and Elm, J.: Contribution of Methanesulfonic Acid to the Formation of Molecular Clusters in the Marine Atmosphere, J. Phys. Chem. A, 126, 7127–7136, 2022.

Riccobono, F., Schobesberger, S., Scott, C. E., Dommen, J., Ortega, I. K., Rondo, L., Almeida, J., Amorim, A., Bianchi, F., Breitenlechner, M., et al.: Oxidation Products of Biogenic Emissions Contribute to Nucleation of Atmospheric Particles, Science, 344, 717–721, 2014.

Rosenfeld, D., Andreae, M. O., Asmi, A., Chin, M., de Leeuw, G., Donovan, D. P., Kahn, R., Kinne, S., Kivek"as, N., Kulmala, M., et al.: Global Observations of Aerosol-Cloud-Precipitation-Climate Interactions, Rev. Geophys., 52, 750–808, 2014.

Rosenfeld, P. E., Henry, C. L., Dills, R. L., and Harrison, R. B.: Comparison of Odor Emissions from Three Different Biosolids Applied to Forest Soil, Water Air Soil Pollut., 127, 173–191, 2001.

Schobesberger, S., Junninen, H., Bianchi, F., L"onn, G., Ehn, M., Lehtipalo, K., Dommen, J., Ehrhart, S., Ortega, I. K., Franchin, A., et al.: Molecular Understanding of Atmospheric Particle Formation from Sulfuric Acid and Large Oxidized Organic Molecules, Proc. Natl. Acad. Sci. U.S.A., 110, 17 223–17 228, 2013.

Schütt, K. T., Kessel, P., Gastegger, M., Nicoli, K. A., Tkatchenko, A., and Müller, K.-R.: SchNetPack: A Deep Learning Toolbox For Atomistic Systems, J. Chem. Theory Comput., 15, 448–455, https://doi.org/10.1021/acs.jctc.8b00908, 2019.

Schütt, K. T., Unke, O. T., and Gastegger, M.: Equivariant Message Passing for the Prediction of Tensorial Properties and Molecular Spectra, arXiv, https://doi.org/10.48550/arXiv.2102.03150, 2021.

Schütt, K. T., Hessmann, S. S. P., Gebauer, N. W. A., Lederer, J., and Gastegger, M.: SchNetPack 2.0: A Neural Network Toolbox for Atomistic Machine Learning, J. Chem. Phys., 158, https://doi.org/10.1063/5.0138367, 2023.

Shen, J., Xie, H.-B., Elm, J., Ma, F., Chen, J., and Vehkamaki, H.: Methanesulfonic Acid-Driven New Particle Formation Enhanced by Monoethanolamine: A Computational Study, Environ. Sci. Technol., 53, 14 387–14 397, 2019.

Shen, J., Elm, J., Xie, H.-B., Chen, J., Niu, J., and Vehkamaki, H.: Structural Effects of Amines in Enhancing Methanesulfonic Acid-Driven New Particle Formation, Environ. Sci. Technol., 54, 13 498–13 508, 2020.

https://doi.org/10.5194/ar-2026-23
Preprint. Discussion started: 24 June 2026

Shen, J., Scholz, W., He, X.-C., Zhou, P., Marie, G., Wang, M., Marten, R., Surdu, M., Rörup, B., Baalbaki, R., et al.: High Gas-Phase Methanesulfonic Acid Production in the OH-Initiated Oxidation of Dimethyl Sulfide at Low Temperatures, Environ. Sci. Technol., 56, 13 931–13 944, 2022.

Sipilä, M., Berndt, T., Pet"aj"a, T., Brus, D., Vanhanen, J., Stratmann, F., Patokoski, J., Mauldin III, R. L., Hyv"arinen, A.-P., Lihavainen, H., et al.: The Role of Sulfuric Acid in Atmospheric Nucleation, Science, 327, 1243–1246, 2010.

Sorooshian, A., Padr'o, L. T., Nenes, A., Feingold, G., McComiskey, A., Hersey, S. P., Gates, H., Jonsson, H. H., Miller, S. D., Stephens, G. L., et al.: On the Link Between Ocean Biota Emissions, Aerosol, and Maritime Clouds: Airborne, Ground, and Satellite Measurements off the Coast of California, Glob. Biogeochem. Cycles, 23, 2009.

Spicher, S., Plett, C., Pracht, P., Hansen, A., and Grimme, S.: Automated Molecular Cluster Growing for Explicit Solvation by Efficient Force Field and Tight-Binding Methods, J. Chem. Theory Comput., 18, 3174–3189, 2022.

Spracklen, D., Carslaw, K., Kulmala, M., Kerminen, V.-M., Mann, G., and Sihto, S.-L.: The Contribution of Boundary Layer Nucleation Events to Total Particle Concentrations on Regional and Global Scales, Atmos. Chem. Phys., 6, 5631–5648, 2006.

VanderGheynst, J. S., Cogan, D. J., DeFelice, P. J., Gossett, J. M., and Walker, L. P.: Effect of Process Management on the Emission of Organosulfur Compounds and Gaseous Antecedents from Composting Processes, Environ. Sci. Technol., 32, 3713–3718, 1998.

Vanhanen, J., Mikkil"a, J., Lehtipalo, K., Sipil"a, M., Manninen, H., Siivola, E., Pet"aj"a, T., and Kulmala, M.: Particle Size Magnifier for Nano-CN Detection, Aerosol Sci. Technol., 45, 533–542, 2011.

Wilemski, G. and Wyslouzil, B. E.: Binary Nucleation Kinetics. I. Self-Consistent Size Distribution, J. Chem. Phys., 103, 1127–1136, 1995.

Wu, H., Engsvang, M., Knattrup, Y., Kubecka, J., and Elm, J.: Improved Configurational Sampling Protocol for Large Atmospheric Molecular Clusters, ACS Omega, 8, 45 065–45 077, 2023.

Wu, H., Knattrup, Y., Jensen, A. B., and Elm, J.: Cluster-to-Particle Transition in Atmospheric Nanoclusters, Aerosol Res. Discuss., 2024, 1–20, 2024.

Zapadinsky, E., Passananti, M., Myllys, N., Kurt'en, T., and Vehkam"aki, H.: Modeling on Fragmentation of Clusters Inside a Mass Spectrometer, J. Phys. Chem. A, 123, 611–624, 2018.

Zhang, J. and Dolg, M.: ABCluster: The Artificial Bee Colony Algorithm for Cluster Global Optimization, Phys. Chem. Chem. Phys., 17, 24 173–24 181, https://doi.org/10.1039/C5CP04060D, 2015.

Zhang, J. and Dolg, M.: Global Optimization of Clusters of Rigid Molecules Using the Artificial Bee Colony Algorithm, Phys. Chem. Chem. Phys., 18, 3003–3010, https://doi.org/10.1039/C5CP06313B, 2016.

Zhao, B., Donahue, N. M., Zhang, K., Mao, L., Shrivastava, M., Ma, P.-L., Shen, J., Wang, S., Sun, J., Gordon, H., et al.: Global Variability in Atmospheric New Particle Formation Mechanisms, Nature, 631, 98–105, 2024.